

## The seismic reliability of two connected SMRF structures

Seyed Bahram Beheshti Aval<sup>\*1</sup>, Amir Farrokhi<sup>1b</sup>, Ahmad Fallah<sup>1c</sup> and Apostolos Tsouvalas<sup>2a</sup>

<sup>1</sup>*Department of Structural Engineering, Faculty of Civil Engineering,*

*K.N. Toosi University of Technology, No. 1346, Vali Asr Street, Mirdamad Intersection, Tehran, Iran*

<sup>2</sup>*Department of Structural Engineering, Faculty of Civil Engineering and Geosciences,  
Delft University of Technology, building 23, Delft, Netherlands*

(Received February 20, 2017, Revised July 5, 2017, Accepted July 10, 2017)

**Abstract.** This article aims to investigate the possible retrofitting of a deficient building with soft story failure mode by connecting it to an adjacent building which is designed based on current code with friction dampers at all floors. Low cost and high performance reliability along with significant energy dissipation pertaining to stable hysteretic loops may be considered in order to choose the proper damper for connecting adjacent buildings. After connecting two neighbouring floors by friction dampers, the sliding forces of dampers at various stories are set in two arrangements: uniform sliding force and then variable sliding force. In order to account for the stochastic nature of the seismic events, incremental dynamic analyses are employed prior and after the installation of the friction dampers at the various floors. Based on these results, fragility curves and mean annual rate of exceedance of serviceability and ultimate limit states are obtained. The results of this study show that the collapse mode of the deficient building can affect the optimum arrangement of sliding forces of friction dampers at Collapse Prevention (CP) performance level. In particular, the Immediate Occupancy (IO) performance level is not tangible to the sliding force arrangement and it depends solely on sliding force value. Generally it can be claimed that this rehabilitation scheme can turn the challenge of pounding two adjacent buildings into the opportunity of dissipating a large amount of the seismic input energy by the friction dampers, thus improving significantly the poor seismic performance of the deficient structure.

**Keywords:** coupled buildings; friction damper; incremental dynamic analysis; fragility curve; mean annual frequency

### 1. Introduction

The collision of neighboring buildings that usually happens in densely populated urban areas during seismic events is recognized as a major source of inducing severe damages to buildings (Fig. 1(a)). The design building codes usually prescribe a minimum separation distance between adjacent buildings to prevent this phenomenon, so one is left with the task of the dynamic analysis of structurally independent units subjected to ground motion excitation. The several reasons, such as, lack of regarding admissible gap, variability in future earthquakes and uncertainties in material properties, and disregarding soil-structure interaction would be claimed for this unfavorable phenomenon. Inter-building pounding may cause serious structural and non-structural damages. Thus, over the last few decades seismic pounding between closely adjacent buildings has been one of the major challenges in earthquake engineering (Bertero and Collins 1973, Penzien 1996, Jankowski and Mahmoud 2016).

Interconnecting adjacent structures with active, semi-active and passive damping devices may be seen as an

opportunity to resolve destructive impact of collision (Iwanami *et al.* 1986, Luco and Debarros 1998, Zhu and Huang 2011).

Installing dampers as connectors between adjacent buildings not only serves as a lateral support system for adjacent buildings but also as a source of energy dissipation during lateral excitation. Turning the challenge of seismic pounding between adjacent buildings into an opportunity of dissipating large amounts of seismic energy and hence causing the buildings to remain damage-free, are the main advantages of application of this method in a rehabilitation programme. Placing such tools does not require extra spaces; since existing space between adjacent buildings may be sufficient.

For example recent application of this technique in connecting flexible adjacent buildings with active dampers was accomplished in 2001 in the Triton Square office complex in Tokyo, Japan (Fig. 1(b)). These 45-, 40- and 35-story adjacent buildings were connected and linked nearby the top floors with 35-ton actuators (Christenson *et al.* 2007). With this method, the initially dynamic independent units are coupled into a single dynamic system and as a result, the response of whole system during seismic excitation is reduced. The paradigm of coupling adjacent buildings was first suggested to control building collision subjected to wind load (Gurley *et al.* 1994, Nigdeli *et al.* 2014).

Performing a literature survey on this subject indicated that pioneer researchers recommended installing semi-

\*Corresponding author, Associate Professor

E-mail: beheshti@kntu.ac.ir

<sup>a</sup>Ph.D.

<sup>b</sup>Ph.D. Student

<sup>c</sup>M.Sc

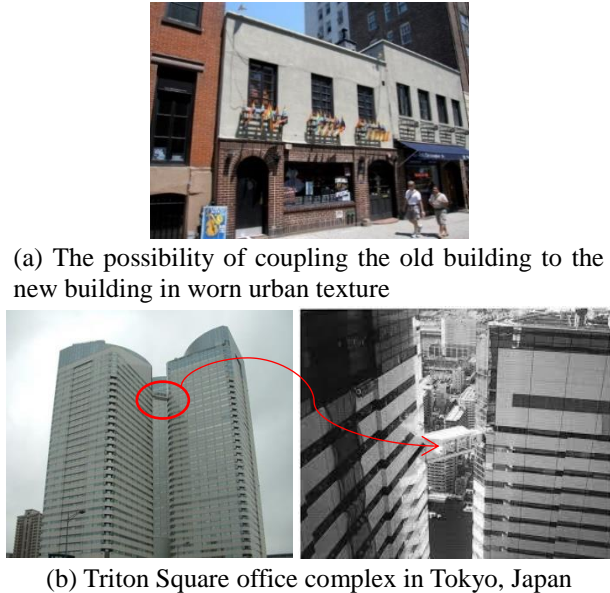


Fig. 1 connecting adjacent buildings in a rehabilitation or new construction program

active damping devices between adjacent structures to mitigate the responses against wind loads are Klein *et al.* (1972). They first designed a semi-active control system in the principal translational direction of a building against wind load. Such systems were shown to have minor (or negligible) effects on the vibrations in the orthogonal directions. In cases where the principal directions were coupled, through connecting two adjacent buildings by cables or other dissipating devices in one direction, the absorption of energy in the other directions was also possible.

In the last two decades a variety of energy dissipation devices were suggested as connectors by researchers. The fluid and viscoelastic dampers were used to reduce dynamic responses of connected buildings and hence improve their seismic performances (Xu *et al.* 1999, Yangt *et al.* 2003, Kima and Ryua 2006).

The semi-active magneto rheological (MR) dampers were examined to mitigate seismic responses of adjacent buildings (Bharti *et al.* 2010, Uz and Hadi 2014, Ketabi *et al.* 2016). Bharti *et al.* utilized a couple of controlling strategies to mitigate seismic response of both adjacent buildings. They concluded that the MR damper was an effective device to reduce the response of both the buildings for various earthquake intensities. Also Abdeddaim *et al.* (2017) used the magneto-rheological (MR) dampers as the semi-active control system for retrofitting of buildings. In their research a ten story feeble building is connected to an adjacent potent building by using MR dampers. They compared their control scheme against passive-on and passive-off control strategies. By applying all three control strategies, pounding mitigation was also studied between two adjacent structures. They resulted that there exists a natural frequency ratio of two adjacent buildings for which utmost control of the feeble structure response takes place with no penalty on the potent structure. This research was shown that connecting adjacent buildings with MR damper

ameliorates the eventuality of pounding mitigation. In another research the MR damper was used to connect the top floors of two ten-story buildings with different dynamic proprieties. This scheme significantly reduces displacement, acceleration and inter-story drift of adjacent buildings. Fuzzy logic controller was used to optimize the magneto-rheological damper force in this research (Abdeddaim *et al.* 2016a, b).

Uz and Hadi (2014) used an optimal design paradigm to reduce seismic responses and also minimize the total cost of hysteretic dampers installed between two adjacent buildings. Their research was based on integrated fuzzy logic and multi-objective genetic algorithm. They concluded that reducing the number of dampers was more effective in the dynamic response of the total system.

The influence of passive viscous and Maxwell dampers as connectors on seismic response of adjacent MDOF structures was studied by Patel and Jangid (2010a, b, 2011). The optimum damper parameters and their positioning on the response of the adjacent structures were evaluated. The same result obtained by Uz and Hadi (2014) in reducing the cost of dampers through selecting the optimal locations of dampers was achieved.

To improve seismic performance of two similar adjacent structures, Park and Ok (2015) studied the hybrid control approach resulting from their coupling. They used passive dampers as connectors and the active control devices were installed as tendon-type devices between two successive five floors in the buildings. The results of analytical model revealed the superiority of proposed system in terms of cost control as well as the proper performance. In a recent work of Palacios-Quiñonero *et al.* (2014), a new structural vibration control strategy was proposed. To this end the local velocity-feedback energy-to peak controller was designed. The success of the new controller through numerical model was indicated.

Due to distinctive advantages of friction dampers, various researchers focused on the application of these well-recognized devices for connecting adjacent buildings (Fig. 2) (Ng and Xu 2004, Bhaskararao and Jangid 2006a, b, Shrimali and Dumne 2008, Patel and Jangid 2010c, Lee *et al.* 2015). These displacement-dependent energy dissipation dampers with rectangular hysteresis loops cause large amount of earthquake energy dissipated through relative sliding of two contacting surfaces (Filiatralt *et al.* 2000). When there is relative movement between similar stories, it is called that stories are in sliding mode, otherwise stories are in non-sliding mode while reaction between connected floors exceeds threshold sliding force value. Friction mechanisms are modelled as springs with a very high stiffness in the non-sliding mode and with (almost) zero stiffness in the sliding mode. It should be noted that slide occurs when applied force exceeds a predefined threshold value (Bhaskararao and Jangid 2006).

Some well-known benefits of using friction dampers are: (i) simple assembly and resistance against failure, (ii); Low-cost and low-tech manufacturing; (iii) acceptable performance against moderate to strong earthquakes; (iv) dissipation of large amount of energy for a given sliding force; (v) performing complimentary damping and

increasing stiffness to improve stability; (vi) no need to repair and replace after major seismic events; (vii) the possibility of controlling sliding force; (viii) their performances are not affected by fatigue phenomena, and ambient temperature and characteristics of excitations (amplitudes, frequencies etc.).

In an experimental evidence, Ng and Xu (2004) implemented a passive friction damper to couple a scaled 12-story steel structures and 3-story podium structure at the level of the third floor. The results were compared against

those of uncoupled and rigid connection cases.

The absolute acceleration and inter-story drift responses of both buildings in case of using friction damper was reduced in comparison to other cases.

In research works of Bhaskararao and Jangid (2006a, b), the friction dampers were installed between two adjacent Multi-Degree-of-Freedom buildings. The almost same reduction in responses was observed while using half the total number of dampers with respect to complete number of them, hence leading to cost reduction.

Using the semi-active variable friction damper (SAVFD) for connecting the two adjacent buildings with different fundamental frequencies in reduction of their responses was studied by Shrimali and Dumne (2008), Patel and Jangid (2010c) and Jagadish and kori (2008). The gain multiplier which was defined as the ratio of damper force (slip force) to critical damper control force was used to study the effectiveness of proposed control strategy in reduction of responses. The effectiveness of proposed SAVFD control strategies was reported. Also the same results of Bhaskararao and Jangid (2006a, b) in reduction of responses were observed when using only 50% of the total number of dampers between adjacent buildings.

As can be seen most published research works were pertaining to installation of dampers between two adjacent similar elastic shear-type structures in order to reduce their responses. The studies focused on assumption of dissipating whole seismic energy in damper devices and nonlinearity in adjacent structures has not been considered under strong earthquake ground shakings. In a rehabilitation programme this method is promising in view of uninterrupted operation/serviceability and also maintained finishing during rehabilitation of adjacent buildings which were inappropriately designed or designed based on older versions of national building codes. Generally many deficient buildings in urban worn area or local historic districts may not have a potential to perform repair scheme against seismic loading. The hospitals or buildings attributed to electricity, gas, and water distribution networks and telecommunication which needs continuous operation are the other examples of these types of buildings. In these cases connecting adjacent structures can be considered as a solution to mitigate the responses of one or both structures against earthquake ground motions. However, such a task should be undertaken very seriously by examining the performance of the individual structures prior and after installation of the dampers at the various floors. This study focuses on this aspect.

No research has been done on seismic reliability evaluation of deficient adjacent buildings before and after connection with dampers. In the present study the probabilistic seismic performance evaluation of two adjacent SMRF structures, connected with friction dampers, is investigated. The outcome provides useful information regarding the performance based seismic risk analysis of two adjacent structures connected with friction dampers and also introduces the rehabilitation of a deficient building while constructing new adjacent building in densely inhabited districts in urban area.

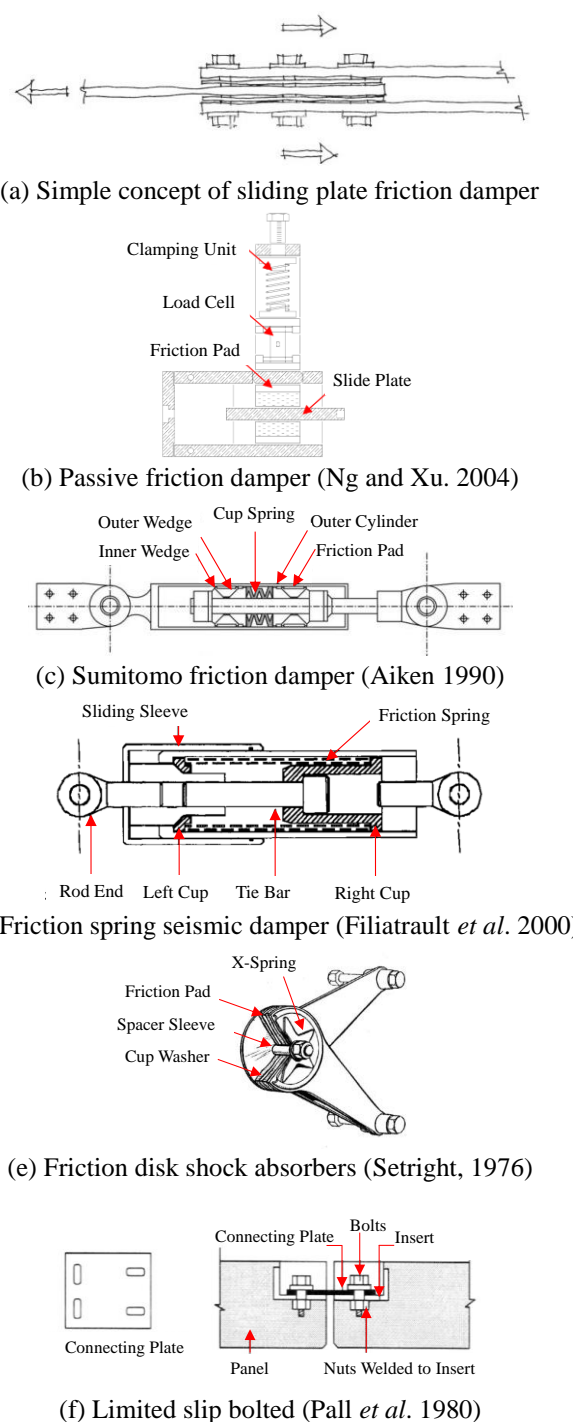


Fig. 2 Diagrammatic view of a couple invented friction dampers

Table 1 Member sections used in buildings

structure	Beams and columns	First story	Second story	Third story	Fourth story
Structure-1 (code- confirming)	beams	IPE 27	IPE 27	IPE 27	IPE 27
	Exterior columns	TUBO 200*200*12.5	TUBO 200*200*12.5	TUBO 200*200*12.5	TUBO 200*200*12.5
	Interior columns	TUBO 160*160*10	TUBO 160*160*10	TUBO 160*160*10	TUBO 160*160*10
Structure-2 (deficient)	beams	IPE 27	IPE 27	IPE 27	IPE 27
	Interior and Exterior columns	TUBO 140*140*8	TUBO 140*140*8	TUBO 140*140*8	TUBO 140*140*8

## 2. The case study and analytical model

The reference prototype adjacent buildings studied in this paper are hypothetically located in Tehran-Iran. However the methodology and results obtained are applicable to the other sites with similar hazard level and soil types. The two buildings have similar plan. They are 4-story/ 3-bay SMRFs in two perpendicular directions (Fig. 3). The story height and bay width are assumed to be 3.2 and 5 meters, respectively. The floors and roof are assumed rigid in-plane, i.e., diaphragmatic behavior (one-way joist floor system). The adjacent building which is called here “code-conforming building” consists of special moment resisting frames, seismically designed according to Iranian Seismic Code (Standard No. 2800, 2007).

The dead load is taken equal to  $5 \text{ kN/m}^2$ , live load for floors and roof equal to  $2 \text{ kN/m}^2$  and  $1.5 \text{ kN/m}^2$ , respectively.

Both structures have residential usage with importance factor of 1. The strength of steel material is 240 MPa (ST-37). According to Iranian seismic code (Standard-2800), the soil type is II with shear wave velocity of  $375 \frac{\text{m}}{\text{s}} < V_s < 750 \frac{\text{m}}{\text{s}}$ . The buildings are located in the highest seismic hazard zone (zone 1) which is equal to the peak ground acceleration of 0.35 g. Also response modification factor for special moment resisting frame systems is considered equal to 8. Design of code-conforming structure (structure-1) is fully performed based on current Iranian design building codes. While the certain value (about %30 obtained from trial and error approach) of base shear of deficient structure

(structure-2) is added to its base shear.

The natural periods of structure-1 and structure-2 obtained from an Eigen value analysis, are 1.080 and 1.308, respectively. Obviously, this certain fraction of base shear needs extra research work, which is beyond the scope of this study. In design of deficient structure the rule of weak beam-strong column strength was not deliberately applied, so the plastic hinge may be induced at columns ends. The difference in stiffness and nonlinear deformation behavior of two assumed adjacent structures cause the proper function of friction dampers between them in both linear and nonlinear deformation range. In Table 1. final sections of beams and columns for both structures are shown.

Since the building is assumed to be symmetric in plan, consideration of a two-dimensional frame to evaluate seismic demand is allowed. Numerical modelling of the sample interior frame of a series of identical frames is implemented using OpenSees software platform (Open Sees 2008). Concentrated plasticity is assumed through assignment of nonlinear rotational springs at beam and column ends with modified Ibarra-Medina-Krawinkler (IMK) moment-rotation model. The backbone curve and hysteresis model of IMK illustrated in Fig. 4(a) (Ibarra *et al.* 2005). Using the hysteresis backbone curve determines its related strength and deformation limitation. The main parameters of the backbone curve in IMK model include the initial stiffness ( $K_e$ ), yield strength ( $M_y$ ), stiffness of hardening branch ( $K_h = \alpha K_e$ ), maximum strength ( $M_c$ ) and its corresponding displacement ( $\theta_c$ ), post-capping stiffness point ( $K_c = \alpha K_e$ ), and residual strength ( $M_r$ ) and its corresponding displacement ( $\theta_r$ ). The capacity coefficient of dissipated hysteresis energy is determined by laboratory data (Lignos 2008). The case study connected frames and panel zone model considered in analyses are shown in Fig. 4(b).

By performing a nonlinear static analysis, plastic hinge locations for both structures corresponding to 3% drift limit state are shown in Fig. 5.

It can be seen that the soft story mechanism is triggered at first story for deficient structure (Structure-2) and induced plastic hinges at beam ends for Structure-1 confirms the application of weak beam-strong column rule.

## 3. Selection of recorded accelerograms

To consider record-to-record variability, Incremental Dynamic Analyses (IDA) is performed for seismic

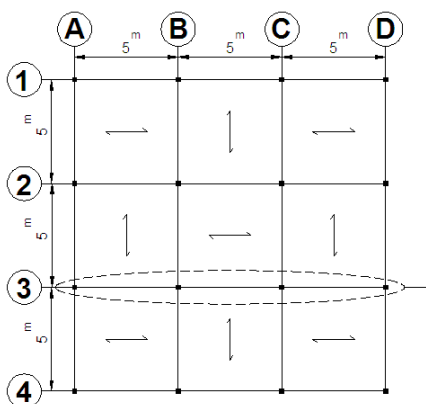
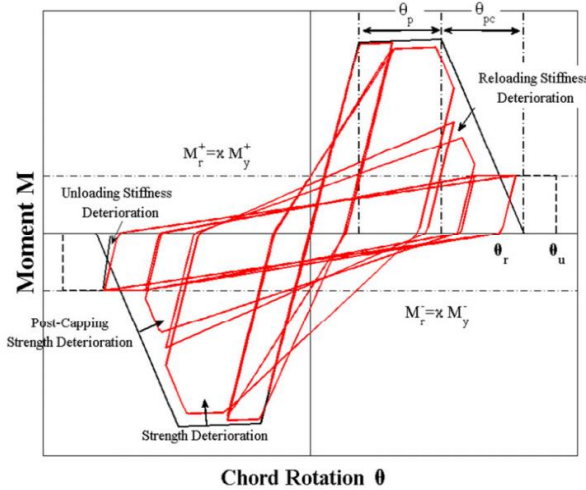
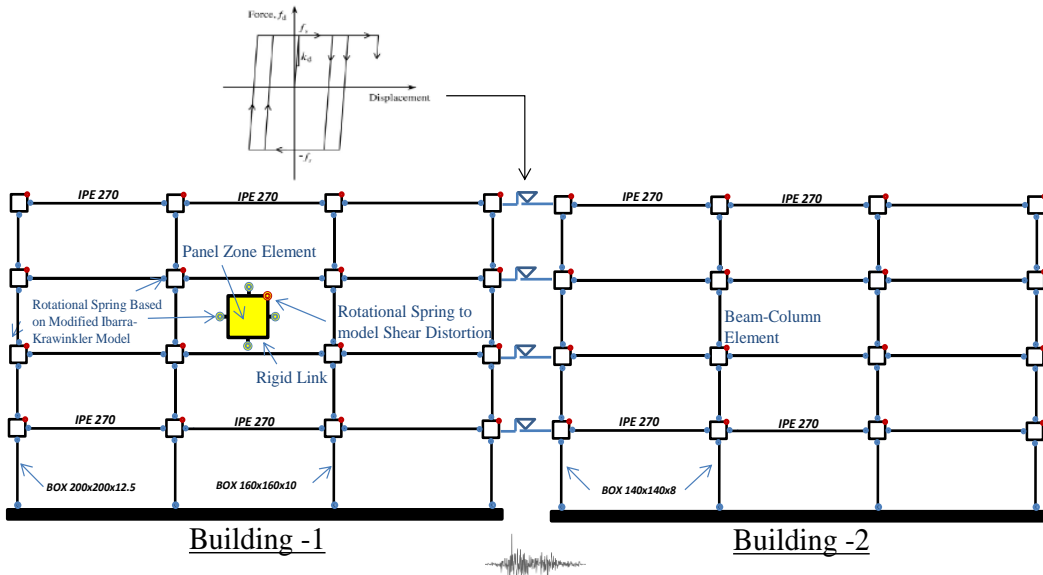


Fig. 3 Plan dimensions and gravity load distribution of adjacent SMRF buildings



(a) The backbone curve and hysteresis model of IMK (Lignos 2008)



(b) Analytical model of two coupled structures connected with friction dampers and M2-WO panel zone

Fig. 4 The frames' models of the case study structures

performance evaluation of structures. A set of 20 earthquake records compatible with seismic hazard at site in Tehran city is chosen. The magnitude, source-to-site distance, soil type and frequency content are compatible with the site-specific acceleration spectrum for the location of interest. Increasing the number of the accelerograms reduces the record to record variability effect and inherent uncertainty of future earthquake characteristics. Earthquake records that are selected for analysis are presented in Table 2. The response acceleration spectra of the scaled records to  $PGA=1.0$  g are shown in Fig. 6. This figure shows that the selected accelerograms have similar frequency contents in wide range of structural deformation.

#### 4. Seismic probabilistic assessment of two separate buildings

The responses of structures under ground motion

excitations are captured through application of IDA method. Each IDA curve is prepared by several nonlinear dynamic analyses of structure, while it is affected by increasing intensities of strong ground motions. These curves represent structural response parameter, entitled as Engineering Demand Parameter (EDP), versus characteristics of affecting strong ground motions, entitled as Intensity Measure (IM). From various possible selection of IM and EDP parameters, the 5% damped acceleration response spectrum at the fundamental period of structure ( $S_a(T)$ ) and the maximum inter-story drift ratio ( $\theta_{max}$ ) are chosen as IM and EDP parameters, respectively. The results of previous studies show the efficiency and sufficiency of these parameters in application of IDA for developing fragility curves (Vamvatsikos and Cornell 2005).

IDA is a regular method in estimating fragility curves for various limit states (Pujari *et al.* 2013, Beheshti Aval *et al.* 2014a, Asgarian *et al.* 2016). The structural fragility for

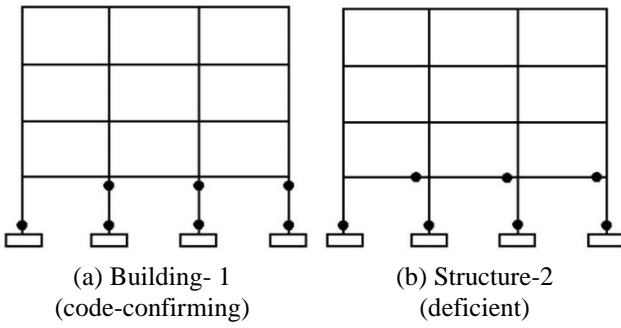


Fig. 5 Failure mechanisms (plastic hinges)

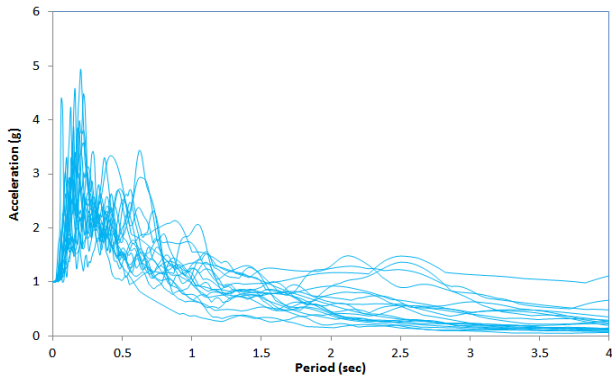


Fig. 6 Scaled acceleration response spectra of selected recorded accelerograms

a limit state which is defined as probability of exceedance of specified damage limit-state is given as Eq. (1)

$$f = P(DS \geq ds | IM = im) \quad (1)$$

In which DS is damage limit-state and ds is the damage amount in structure.

Estimation of fragility curves can be stated according to EDP or IM approaches. In IM-Based approach for derivation of fragility curves, IM (usually selected as spectral acceleration) is selected as the variable for determination of limit-state; thus probability of collapse can be stated as Eq. (2)

$$P(C|IM = im_i) = P(im_i > IM_c) = F_{IM_c}(im_i) \quad (2)$$

In the equation above,  $F_{IM_c}(im_i)$  denotes the cumulative distribution function of IM (here, spectral acceleration) capacity. Because of intrinsic randomness of earthquakes, IM varies from one record to another record. This method is usually used for developing collapse fragility curves and cannot be used for other limit states. IM corresponding to collapse occurs when IDA curve resulting from nonlinear response history analysis shows non-convergence (i.e., dynamic instability is attained) within a certain tolerance; which is pertaining to P-Δ effects and also strength and stiffness degradation of structural components (Beheshti Aval *et al.* 2014b).

In EDP-Based approach for estimating fragility curves, an EDP is used as the variable for determination of a certain limit-state. At each specified intensity (hazard level),

various EDPs would be obtained regarding record-to-record variability. It means that each line attributed to certain intensity which is parallel to EDP axis crosses IDA curves at various EDPs. Estimating EDPCs at two limit states were collected from SAC/FEMA recommendation for SMRF structures (FEMA 350, 2000). For Immediate Occupancy (IO) (serviceability) and Collapse Prevention (CP) (safety) performance level attaining EDP of 2% and 10% maximum inter-story drift ratio were considered, respectively. In CP, additional criteria of EDP value at which the slope of the IDA curve becomes less than 20% of the initial elastic slope of IDA curve was adjoined. The mathematical description of EDP-Based approach is shown in Eq. (3). (Zarein *et al.* 2010, Baker 2015, Lee *et al.* 2014)

$$\begin{aligned} P(C|IM = im_i) &= P(EDP_d > EDP_c | IM = im_i) = \\ &\sum_{\text{all } edp_c} P(EDP_d > EDP_c | EDP_c = edp_{ci}), \quad (3) \\ &IM = im_i \times P(EDP_c = edp_{ci}) \end{aligned}$$

Thus for a specified  $edp_{ci}$ ,  $P(EDP_c = edp_{ci})$  and  $P(EDP_d > EDP_c | EDP_c = edp_{ci})$  at any level of  $im_i$  can be calculated. Then through summation of derived probabilities for all  $edp_{ci}$ ,  $P(C|IM = im_i)$  would be obtained.

To capture fragility curve at CP and IO performance level, IM and EDP approaches are utilized, respectively. After conducting multiple response history analyses for each accelerogram at various intensity levels, the output  $\theta_{\max}$  is obtained. To easily summarize the IDA curves into central value and a measure of dispersion, the 16th, 50th, and 84th percentiles of resulted IDAs for two structures are shown in Fig. 7. The greater strength and ductility capacity can be seen for code-confirming building in comparison with deficient building. Fragility curves can also be depicted in Fig. 8 which is the outcome of IDA results for both buildings.

Based on statistical determination of data obtained from IDA curves, the fragility curves are obtained for two limit states i.e., IO and CP.

These graphs show that in both limit states, the damage probability of Structure-1 in a wide range of intensity is much lower than Structure-2.

## 5. Optimum sliding force optimum

All previous analyses are repeated for coupled buildings with friction dampers. The most important characteristic parameter of friction damper is its sliding force. The sliding force refers to the maximum resistance created when the two surfaces slide against each other. In other words, after imposing force larger than the sliding force, the two surfaces slide with respect to each other and the damper absorbs part of the kinetic energy by converting it into thermal energy. In order to obtain the optimum sliding force for each earthquake record, a time history analysis performed. In this process, sliding force of damper ( $f_s$ )

Table 2 Selected acceleration for IDA

N.	Earthquake	Station	Comp	Mw	R (km)	PGA (g)
1	Cape Mendocino,1992	Fotuna Blvd.	0	7.1	23.6	0.116
2	Hollister,1986	Hollister, Diff Array #1	125.5	5.4	16.9	0.101
3	Landers,1992	Barstow	0	7.3	36.1	0.132
4	Loma Prieta,1989	Coyote Lake Dam,DOWN	195	6.9	22.3	0.160
5	San Fernando,1971	Whittier Narrows Dam	233	6.9	45.1	0.107
6	Northridge,1994	LA, Saturn St.	20	6.7	30.0	0.474
7	N. Palm Springs,1986	Indio	315	6.0	39.6	0.117
8	Superstition Hills(A),1987	Wildlife Liquefaction Array	360	6.3	24.7	0.134
9	Loma Prieta,1989	Agnews State Hospital	90	6.9	28.2	0.159
10	Northridge,1994	24303 LA - Hollywood	90	6.7	25.5	0.231
11	Imperial Valley,1979	Compuertas	285	6.5	32.6	0.147
12	Imperial Valley,1979	Plaster City	135	6.5	31.7	0.057
13	Imperial Valley,1979	El Centro Array #12	140	6.5	18.2	0.143
14	Loma Prieta,1989	Anderson Dam	360	6.9	21.4	0.240
15	Imperial Valley,1979	Chihuahua	12	6.5	28.7	0.270
16	Imperial Valley,1979	El Centro Array #13	140	6.5	21.9	0.117
17	Imperial Valley,1979	Westmorland Fire Station	90	6.5	15.1	0.074
18	Superstition Hills(B),1987	Wildlife Liquefaction Array	90	6.7	24.4	0.181
19	Mt .Lewis,1986	Halls Valley	90	5.6	15.5	0.159
20	Kern County,1952	Holywood Stor Lot	90	7.4	20.5	0.042

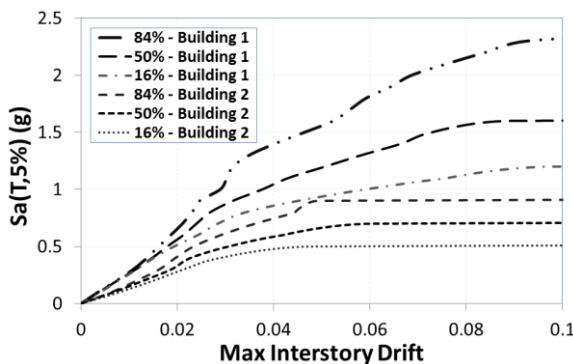
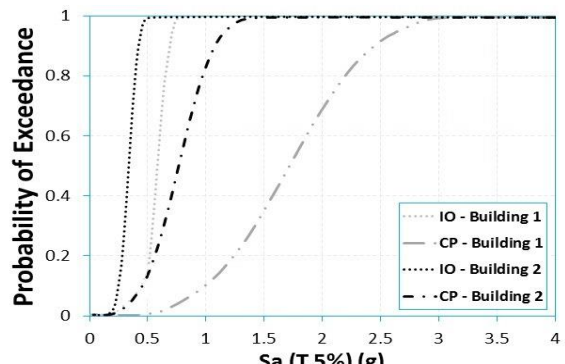
Fig. 7 16<sup>th</sup>, 50<sup>th</sup>, and 84<sup>th</sup> percentiles of IDA curves for two separate buildings

Fig. 8 Fragility curves of two buildings at two limit state levels

varies between 0 to 5 kN. For each analysis, maximum displacement of the roof and the base shear are recorded.

In order to obtain the optimum sliding force, the mean value of the roof displacement and the shear base is plotted against the sliding force. Also Square Root of Sum of Squares (SRSS) of each response is plotted. The SRSS is used here to represent the mean values of responses of two adjacent buildings as a whole system. In process of deriving the optimum sliding force, the minimum SRSS is concerned. Obviously the optimum sliding forces of friction dampers is an optimization problem which depends on several parameters such as the relative stiffness/strength of neighboring floors, the type and the inherent specifications of seismic excitations and so on. At first place, all friction dampers installed at all neighboring floors have the same sliding forces. Subsequently, the sliding forces at each floor

level are considered proportional to the story shear forces. Obtaining optimum variations of sliding forces at various floor levels is beyond the scope of this study and will be the extension of this research work.

For comparative illustration of the effect of connecting two adjacent buildings, the time-history of responses such as roof displacement and base shear prior and after connecting subjected to all seismic records of Table 2, are computed and for instance the time-history of responses for a sample earthquake record 7 are shown in Fig. 9. These figures clearly show the influence of dampers in reducing both roof displacements and base shear forces.

### 5.1 Connection adjacent buildings with dampers having uniform sliding force at floors (Uniform-damping scheme)

Table 3 Seismic response of both structures to earthquakes before and after connecting in uniform-damping scheme

Earthquake	Building 1						Building 2					
	Top Floor Disp. (cm)			Base Shear (kN)			Top Floor Disp. (cm)			Base Shear (kN)		
	Before connecting	After connecting	Percentage of Reduction	Before connecting	After connecting	Percentage of Reduction	Before connecting	After connecting	Percentage of Reduction	Before connecting	After connecting	Percentage of Reduction
Cape Mendocino,1992	6.57	7.04	-7.17	11.45	12.78	-11.66	8.49	7.47	11.97	12.02	8.16	32.10
Hollister,1986	2.33	2.58	-10.58	5.01	5.18	-3.52	3.98	2.50	37.32	6.55	2.74	58.13
Landers,1992	6.49	5.59	13.97	11.82	10.87	7.97	6.87	6.22	9.47	9.44	5.90	37.54
Loma Prieta,1989	5.49	5.40	1.77	12.10	10.81	10.67	7.88	5.73	27.26	10.22	7.28	28.80
San Fernando,1971	2.22	2.21	0.65	3.96	5.34	-34.97	4.37	2.25	48.57	5.03	3.16	37.22
Northridge,1994	9.92	8.16	17.82	21.43	14.82	30.87	11.22	8.64	22.95	15.50	12.06	22.20
N. Palm Springs,1986	7.89	5.51	30.14	15.66	12.06	23.03	10.46	6.36	39.21	11.68	6.64	43.12
Superstition Hills(A),1987	4.16	4.73	-13.73	7.74	8.85	-14.27	7.47	5.10	31.71	8.26	5.30	35.87
Loma Prieta,1989	4.86	5.48	-12.77	10.31	11.27	-9.29	8.68	7.15	17.56	10.65	7.48	29.73
Northridge,1994	11.06	9.67	12.53	21.48	16.36	23.84	12.44	10.45	16.02	13.13	10.52	19.84
Imperial Valley,1979	1.97	2.02	-2.89	4.37	3.98	9.00	2.75	1.99	27.56	2.81	2.23	20.67
Imperial Valley,1979	1.39	1.55	-11.17	3.31	3.72	-12.42	3.43	1.95	43.00	3.98	2.08	47.78
Imperial Valley,1979	8.02	6.80	15.21	18.00	16.34	9.21	10.94	7.70	29.63	12.52	8.93	28.66
Loma Prieta,1989	5.23	5.81	-11.10	12.47	12.76	-2.30	10.96	7.29	33.53	11.91	8.44	29.15
Imperial Valley,1979	9.41	7.61	19.14	17.75	16.11	9.25	12.42	9.08	26.95	11.62	9.30	19.98
Imperial Valley,1979	5.33	4.45	16.58	10.01	9.36	6.55	6.77	4.89	27.83	8.17	5.00	38.82
Imperial Valley,1979	3.39	3.02	10.73	7.49	7.05	5.82	5.37	3.29	38.62	6.92	4.54	34.43
Superstition Hills(B),1987	10.20	8.74	14.26	19.71	17.32	12.17	14.69	10.45	28.87	13.45	10.92	18.84
Mt. Lewis,1986	7.84	8.46	-7.89	15.54	16.24	-4.47	11.70	10.68	8.70	11.81	9.90	16.18
Kern County,1952	2.75	2.91	-5.84	5.70	6.03	-5.72	5.06	3.91	22.62	6.72	4.34	35.38

The mean results of multiple response history analysis lead to an optimum sliding force of 0.4 kN in this case (Fig. 10). At this stage SRSS of the displacements reaches a minimum, after which it becomes constant while the SRSS of the base shear is significantly reduced.

Table 3 shows maximum roof displacements and base shears as well as their percentile reduction before and after connecting the buildings with friction dampers. As can be seen, the mean maximum displacement of the roofs in Structure-1 and 2 are reduced by 3.48% and 27.47%, respectively. Also the mean base shear for Structure-1 and 2 are reduced by 2.49% and 31.72%, respectively. As a result, although the roof displacement and base shear of structure-1 (code-confirming) increases in a couple of records, the response of structure-2 (deficient) and the system as a whole are reduced.

### 5.2 Connection adjacent buildings with dampers having variable sliding force at floors (Linear-damping scheme)

Based on triangular distribution of lateral seismic force recommended in codes (for regular buildings), sliding

forces are reduced at each floor linearly from top to bottom. As a result sliding forces are taken as  $f_s$ ,  $0.75f_s$ ,  $0.5f_s$ , and  $0.25f_s$  from top to bottom.

Referring to Fig. 11, the SRSS of displacement reaches a minimum at a sliding force of 0.6 kN and after that becomes constant. In addition the SRSS of the base shear is considerably reduced. As it can be seen, the average of the optimum sliding force is reduced with respect to uniform height-wise arrangement of sliding force.

Table 4 shows maximum roof displacements and base shears as well as their percentile reduction before and after connecting the two buildings with friction dampers having variable sliding force. As can be seen, the mean maximum roof displacements of buildings 1 and 2 are reduced by 2.28% and 27.66%, respectively. The mean base shears are reduced to 2.65% and 28.94%, respectively.

In comparison with the uniform-damping scheme, inferior performance of the coupled structure is obtained in this case. This result may be explained through the manifestation of the soft first story mechanism of Structure-2 (deficient) and the consequent development of a uniform lateral displacement pattern along the height of the building which, in turn, excites all dampers at a similar rate.

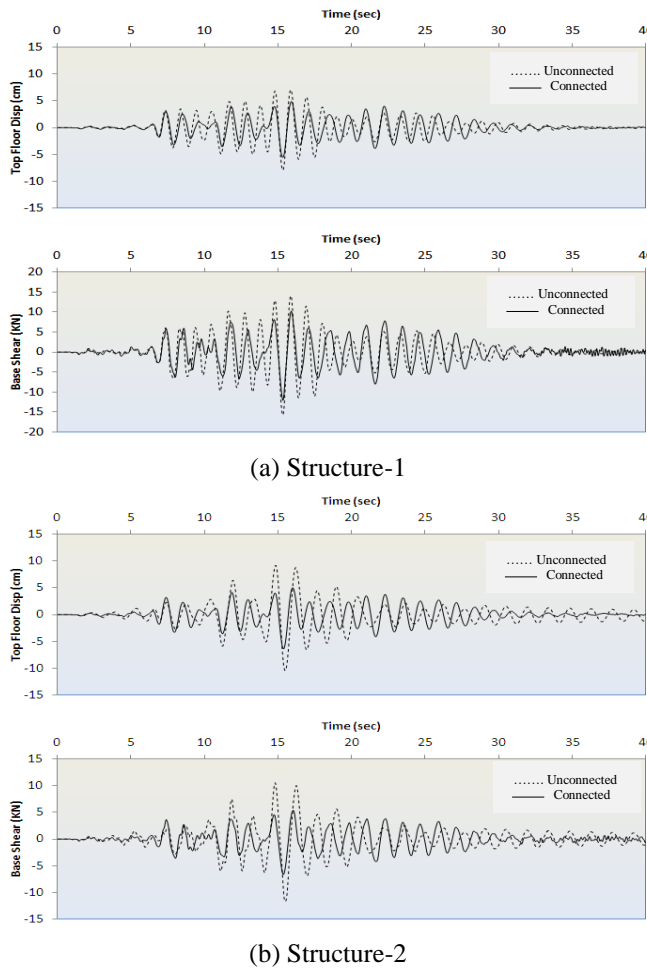


Fig. 9 The comparison of roof displacement/ base shear history under Earthquake record 7 (N. Palm Springs)

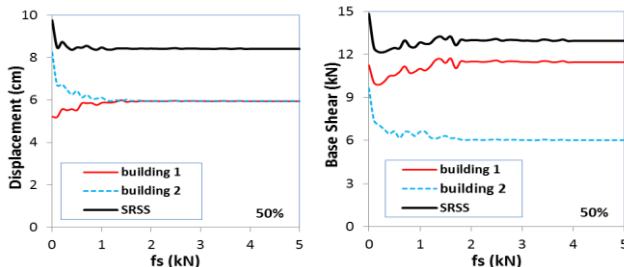


Fig. 10 Displacement and base shear response of two coupled buildings vs. Sliding forces of the dampers (Uniform-damping scheme)

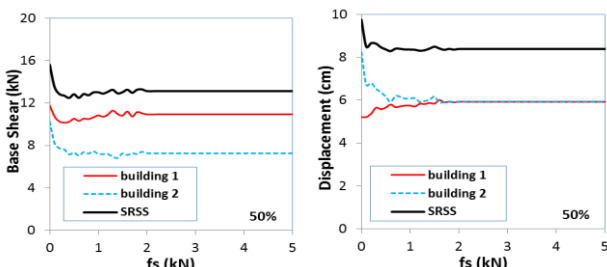


Fig. 11 Displacement and base shear response of the two buildings vs. Sliding forces of the dampers (Linear-damping scheme)

## 6. Limit state probability evaluation of two coupled buildings

### 6.1 Uniform-damping scheme

IDA for two buildings separately and then after connecting with the similar friction dampers was performed and the results in forms of triple-percentile IDA curves (16%-50%-84%) are shown in Figs. 12-13.

Fragility curves of two buildings before and after connecting at two limit states of IO and CP levels are demonstrated in Fig. 12. The probability of exceedance of damages of Structure-1 is increased at IO performance level after connecting to Structure-2 in vast varying intensities. At CP performance level, this depends on intensity level. Under intensity of  $Sa=1.5$  g (lower intensities) the probability is increased and in range of higher values the probability is decreased.

This achievement is mainly attributed to the greater numbers of dampers that are excited, and hence dissipated the larger amount of seismic energy, in range of the higher seismic intensities. In these circumstances, less seismic energy is left to be transferred to the structures which reduces their collapse probabilities.

A limited change in the collapse probability in structure-1 in comparison with those probabilities in structure-2 can be seen. The collapse probability of structure-2 has been considerably reduced with the aid of this type of rehabilitation scheme.

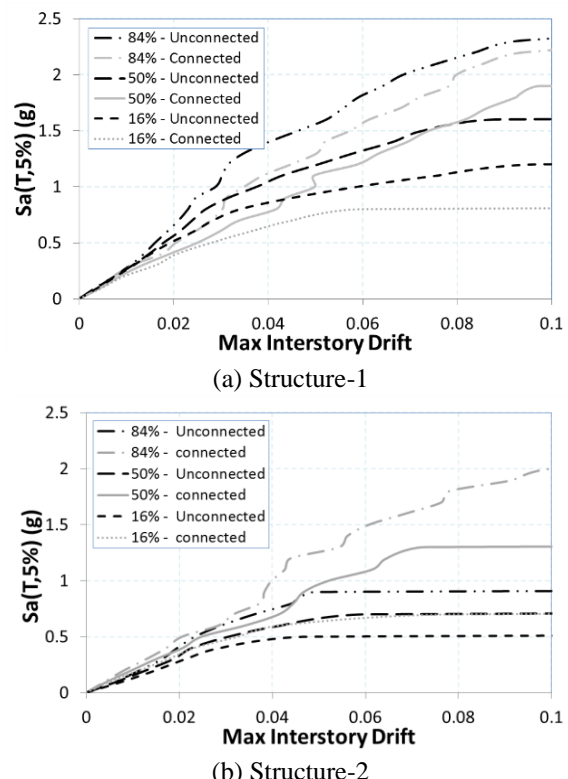


Fig. 12 16<sup>th</sup>, 50<sup>th</sup>, and 84<sup>th</sup> percentiles before and after connecting (uniform-damping scheme)

Table 4 Seismic response of both structures to earthquakes before and after connecting in linear-damping scheme

Earthquake	Building 1						Building 2					
	Roof Disp. (cm)			Base Shear (kN)			Roof Disp. (cm)			Base Shear (kN)		
	Before connecting	After connecting	Percentage of Reduction	Before connecting	After connecting	Percentage of Reduction	Before connecting	After connecting	Percentage of Reduction	Before connecting	After connecting	Percentage of Reduction
Cape Mendocino,1992	6.57	6.99	-6.48	11.45	12.84	-12.14	8.49	7.53	11.29	12.02	8.10	32.59
Hollister,1986	2.33	2.54	-9.15	5.01	4.81	3.94	3.98	2.66	33.11	6.55	2.92	55.51
Landers,1992	6.49	5.61	13.57	11.82	10.58	10.43	6.87	6.13	10.73	9.44	6.26	33.64
Loma Prieta,1989	5.49	5.37	2.21	12.10	10.63	12.13	7.88	5.76	26.93	10.22	7.63	25.35
San Fernando,1971	2.22	2.22	0.35	3.96	5.66	-42.90	4.37	2.28	47.74	5.03	3.44	31.65
Northridge,1994	9.92	7.97	19.65	21.43	15.06	29.75	11.22	8.56	23.69	15.50	11.91	23.14
N. Palm Springs,1986	7.89	5.81	26.39	15.66	12.07	22.93	10.46	5.90	43.60	11.68	6.61	43.42
Superstition Hills(A),1987	4.16	4.81	-15.76	7.74	8.78	-13.43	7.47	5.09	31.83	8.26	5.73	30.63
Loma Prieta,1989	4.86	5.45	-12.11	10.31	11.36	-10.18	8.68	7.25	16.43	10.65	7.74	27.34
Northridge,1994	11.06	9.45	14.57	21.48	15.63	27.23	12.44	10.22	17.85	13.13	10.51	19.92
Imperial Valley,1979	1.97	2.03	-3.05	4.37	3.61	17.27	2.75	2.11	23.23	2.81	2.26	19.48
Imperial Valley,1979	1.39	1.55	-11.15	3.31	3.71	-12.10	3.43	1.95	43.09	3.98	2.29	42.56
Imperial Valley,1979	8.02	6.86	14.49	18.00	16.00	11.14	10.94	7.74	29.24	12.52	9.50	24.15
Loma Prieta,1989	5.23	6.07	-15.94	12.47	13.37	-7.19	10.96	6.67	39.13	11.91	8.31	30.24
Imperial Valley,1979	9.41	8.00	15.01	17.75	16.37	7.78	12.42	9.47	23.76	11.62	10.26	11.70
Imperial Valley,1979	5.33	4.74	10.98	10.01	9.06	9.50	6.77	4.54	33.01	8.17	5.49	32.87
Imperial Valley,1979	3.39	3.12	7.87	7.49	6.86	8.33	5.37	3.26	39.24	6.92	4.98	27.97
Superstition Hills(B),1987	10.20	9.02	11.54	19.71	17.59	10.78	14.69	10.06	31.51	13.45	11.15	17.14
Mt .Lewis,1986	7.84	8.27	-5.50	15.54	15.90	-2.30	11.70	10.85	7.27	11.81	9.62	18.56
Kern County,1952	2.75	3.07	-11.88	5.70	6.72	-17.88	5.06	4.02	20.47	6.72	4.64	31.03

## 6.2 Linear-damping scheme

In the same way the triple-percentile IDA curves and fragility curves for each building separately and after coupling are shown in Figs. 14 and 15.

Similar results were obtained for linear-damping scheme as with the uniform arrangement discussed previously. Again, a considerable reduction in the collapse probability of Structure-2 after coupling is observed. In this case, the threshold intensity is increased to  $S_a=1.75$  g, i.e., in slightly wider intensity, the connecting buildings with dampers

increase the collapse probability of Structure-1.

To better illustrate the comparison of two arrangements, the mean IDA curves and fragility curves are shown together before and after connection in Fig. 16. Generally concluding, at low intensity ranges, the variable damping scheme shows larger capacity with respect to uniform one especially in code-conforming structure (Structure-1).

Albeit direct anchoring a weak structure to a strong one is expected to lead to an overall reduction of the performance of strong one in favor of promoting the performance of the weak one, in case of connecting the

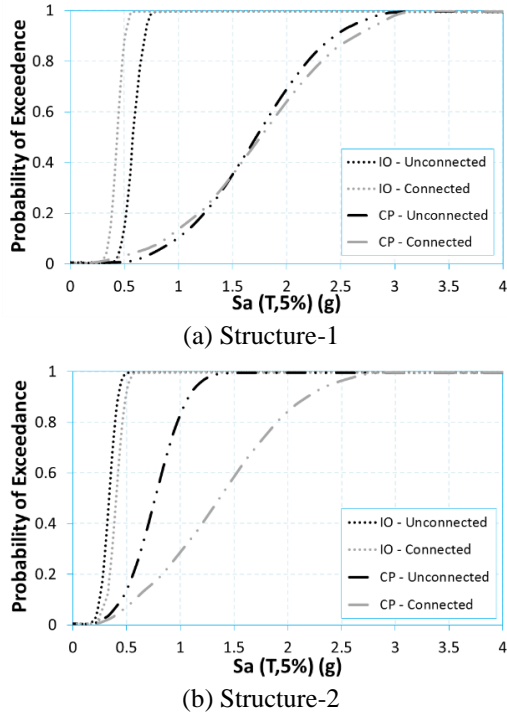


Fig. 13 Fragility curves before and after connecting - (uniform-damping scheme)

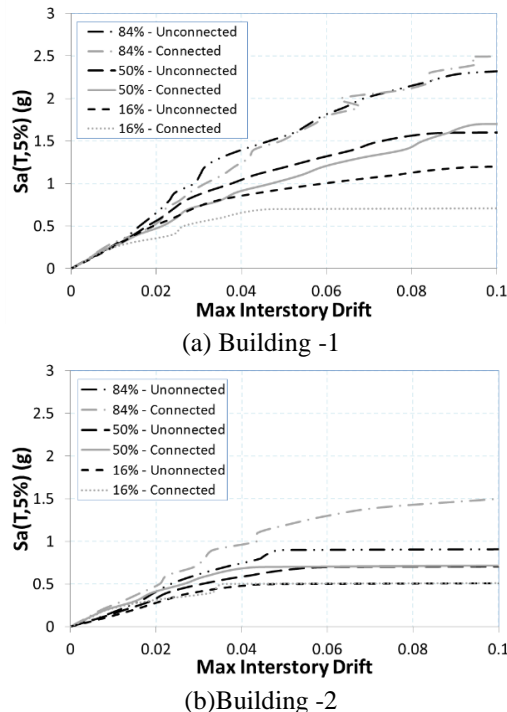


Fig. 14 The comparison of statistical percentiles for building- 1 before and after connecting (linear-damping scheme)

adjacent buildings with friction dampers, a rather surprising achievement at CP level is observed. Depending on the lateral resistance and stiffness level of the strong structure (i.e., predefined initial augmented design base shear which is depend on lateral resistance of adjacent weak structure),

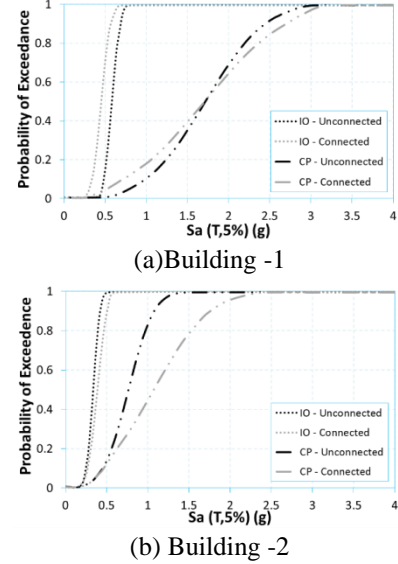


Fig. 15 The comparison of fragility curves before and after connecting (linear-damping scheme)

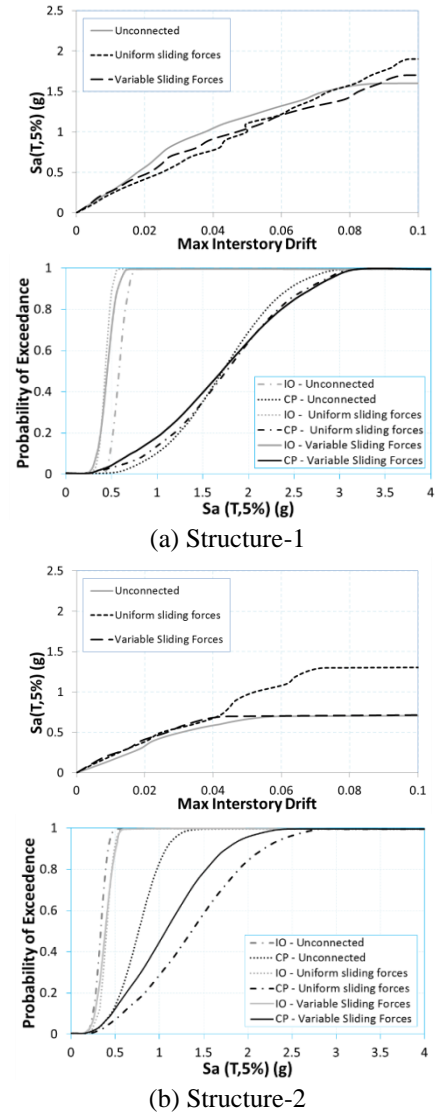


Fig. 16 Mean IDA curves and fragility curves for different scenarios

at range of greater intensity ground shaking level of a specified one (here  $Sa=1.75$  g) connecting adjacent structures improves the performance (reduce collapse probability) of the strong structures in both arrangements of the friction dampers. In this rehabilitation scheme under a strong earthquake excitation, a large amount of the seismic input energy is dissipated in the friction connectors between adjacent buildings.

Thus, based on the results of this study when strong earthquakes are expected, connecting adjacent buildings with friction dampers may be considered as the added value for both structures and not only for the weak ones.

### 6.3 Mean annual occurrence frequency

To include uncertainties of ground motion intensity which are commonly represented by site seismic hazard curve in performance evaluation, the Mean Annual occurrence Frequency (MAF) for two buildings before and after connecting them to each other is calculated. The MAF of exceeding a limit state is computed by integrating the corresponding fragility curve over the mean hazard curve.

MAF formula follows as Eq. (4)

$$\lambda_{LS} = \int_{IM=0}^{IM=\infty} F(IM_c | IM) \cdot \left| \frac{d\lambda_{IM}}{dIM} \right| dIM \quad (4)$$

In which absolute quantity is gradient of hazard function respected to IM, and  $F(IM_c | IM)$  is cumulative distribution function of limit state occurrence capacity based on IM variable. In Eq. (4), the cumulative distribution function is a fragility function. In order to evaluate absolute quantity, seismic hazard analysis for site location should be performed. The results of seismic hazard analysis for Tehran region with 36.37 latitude and 52.33 longitudes has been determined as simple two-parameter equation of Eq. (5) (Jalayer 2003, Wang and Taheri 2014)

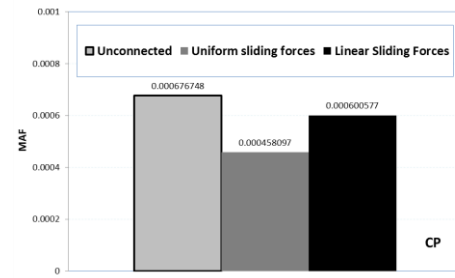
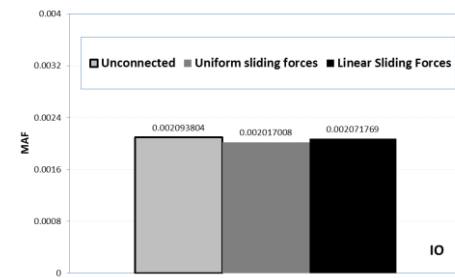
$$\lambda_{Sa} = k_0 (sa)^{-k} \quad (5)$$

The parameters of  $k$  and  $k_0$  for different fundamental periods of structures before and after coupling are presented in Table 5. Substituting Eq. (5) in Eq. (4) and performing numerical integration yields MAF for IO and CP levels.

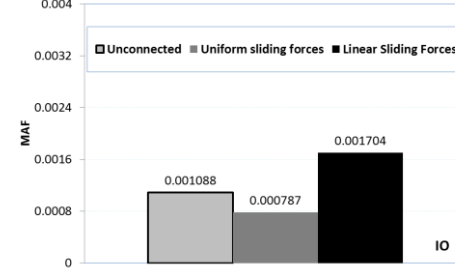
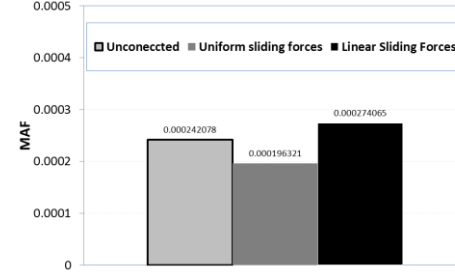
Basically MAF of exceeding a specific limit state is a good index for demonstrating overall performance of the building at various hazard levels. Lower value of MAF shows lower probable performance of a building exceeded from a specific limit state. MAFs for IO and CP levels are shown in Figs. 17 for both buildings separately. Both scenarios of uniform and linear arrangements of dampers cause both predefined performance levels of Structure-2 to be improved after connecting to Structure-1. This improvement is more pronounce at CP level with respect to IO. Comparison of results show that by connecting two buildings with uniform sliding force friction dampers, the buildings' performances improves at both IO and CP levels. By connecting two buildings with linear-damping scheme causes building performance improvement of structure-2 at both IO and CP levels while performance of structure-1 decreases slightly at the CP level and significantly at IO

Table 5 Hazard parameters

		$T_1(\text{sec})$	$k_0$	$k$
Before connection	building 1	1.080	0.00071	2.13490
	building 2	1.308	0.00033	2.03554
After connection	building 1	1.275	0.00030	2.02101
	building 2	1.275	0.00030	2.02101



(a) Structure-1



(b) Structure-2

Fig. 17 MAFs at IO and CP performance levels for different sliding force arrangement of friction dampers

level. In IO performance level, the majority of the dampers were not activated and performed as rigid connecting elements. Thus, the energy absorption in the dampers was limited. In contrast, when the CP performance level is examined, numerous dampers were activated and therefore a larger amount of energy is absorbed due to the larger exploitation of the non-linear responses of the dampers.

It can be concluded that the best performance for both case-studied buildings occurs in uniform-damping scheme in respect to linear scheme. Formation of soft-story-mechanism failure mode at first story which excites friction dampers at all floors (caused to uniform lateral displacement at Structure-2 floors) is probably the underlying cause for the observed behavior.

## 7. Conclusions

In this paper, a probabilistic assessment of the seismic performance of two adjacent buildings separately and after connecting them with friction dampers was studied. Each pair of neighboring floors between a code-conforming and a deficient building is connected with a friction damper. While application of traditional retrofitting schemes of deficient building from a couple of aspects such as economic, service interruption, social and cultural (e.g., for historic buildings) may not be suitable, possibility of retrofitting these buildings by connecting them to existing or newly designed adjacent buildings may be an attractive alternative. Installation of frictional connections causes absorption of earthquake energy and reduces the damage of the deficient building. In this way, extra story-shear forces of deficient building are transmitted to the modern one through friction damper devices acting as lateral supports. The efficiency of two arrangements of dampers is examined through selecting uniform and variable sliding forces at different story levels.

The following conclusions can be drawn. First, regardless of the seismic hazard level at a site, connecting adjacent buildings (attributed to code-conforming and deficient) with friction dampers decreases damage probability of the code non-conforming building while increases it slightly for the code-conforming building in both IO and CP performance levels. This reduction of damage probability in uniform-damping scheme is more pronounce than with linear scheme. Second, considering seismic hazard zone of Tehran, less MAF at both performance levels for both buildings are evaluated in uniform-damping scheme in comparison with linear-damping scheme. Inspection of deformations of both buildings reveals that the formation of a soft-story failure mode at first story of deficient building excites all friction dampers in a uniform-damping scheme. Third, the height-wise arrangement of sliding force friction damper is an optimization problem in which, the relative elastic and post elastic force-deformation relationship of the adjacent floors is critical. Finally, this simple and economic scheme can be suggested as a promising paradigm in rehabilitation program of texture urban worn in view of reducing expenses and implementation time to complete the program in applying to the bunch of deficient buildings.

## References

- Abdeddaim, M., Ounis, A., Shrimali, M.K. and Datta, T.K. (2017), "Retrofitting of a weaker building by coupling it to an adjacent stronger building using MR Dampers", *Struct. Eng. Mech.*, **62**(2), 197-208.
- Abdeddaim, M., Ounis, A., Djedoui, N. and Shrimali, M.K. (2016a), "Pounding hazard mitigation between adjacent planar buildings using coupling strategy", *J. Civ. Struct. Hlth. Monit.*, **6**(3), 603-617.
- Abdeddaim, M., Ounis, A., Djedoui, N. and Shrimali, M.K. (2016b), "Reduction of pounding between buildings using fuzzy controller", *Asian J. Civ. Eng. (BHRC)*, **17**, 985-1005.
- Aiken, I.D. and Kelly, J.M. (1990), "Earthquake simulator testing and analytical studies of two energy-absorbing systems for multistory structures", Earthquake Engineering Research Center (EERC), Report No. UCB/EERC-90/3, University of California at Berkeley, USA.
- Asgarian, B., Salehi Golsefidy, E. and Shokrgozar, H.R. (2016), "Probabilistic seismic evaluation of buckling restrained braced frames using DCFD and PSDA methods", *Earthq. Struct.*, **10**(1), 105-123.
- Baker, J.W. (2015), "Efficient analytical fragility function fitting using dynamic structural analysis", *Earthq. Spectra*, **31**(1), 579-599.
- Beheshti Aval, S.B., Khojastehfar, E., Zolfaghari, M. and Nasrollahzadeh, K. (2014), "Collapse fragility curve development using Monte Carlo simulation and artificial neural network", *J. Risk Reliability*, **228**(3), 301-312.
- Beheshti Aval, S.B., Masoumi Verki, A. and Rastegaran, M. (2014), "Systematical approach to evaluate collapse probability of steel MRF buildings based on engineering demand and intensity measure", *International Conference on Advances in Civil Structural and Mechanical Engineering*, Birmingham, United Kingdom, doi: 10.3850/978-981-07-8859-9\_28.
- Bertero, V.V. and Collins, R.G. (1973), "Investigation of the failures of the Olive View stair-towers during the San Fernando earthquake and their implications on seismic design", Report No. EERC 73-26, Earthquake Engineering Research Center, University of California, Berkeley, USA.
- Bharti, D., Dumne, S.M. and Shrimali, M.K. (2010), "Seismic response analysis of adjacent buildings connected with MR dampers", *Eng. Struct. J.*, **32**(8), 21-22.
- Bhaskar Rao, A.V. and Jangid, R.S. (2006), "Seismic response of adjacent buildings connected with friction dampers", *Bull. Earthq. Eng.*, **4**(1), 43-64.
- Bhaskar Rao, A.V. and Jangid, R.S. (2006), "Harmonic response of adjacent structures connected with a friction damper", *J. Sound Vib.*, **292**(3-5), 710-725.
- Christenson, R., Spencer, B. and Johnson, E. (2007), "Semiactive connected control method for adjacent multidegree-of-freedom buildings", *J. Eng. Mech.*, **133**(3), 290-298.
- FEMA 350. (2000), "Recommended seismic design criteria for new steel moment-frame buildings", Washington, DC: SAC Joint Venture, Federal Emergency Management Agency.
- Filiatrault, A., Tremblay, R. and Kar, K. (2000), "Performance evaluation of friction spring seismic damper", *J. Struct. Eng.*, **126**(4), 491-499.
- Gurley, K., Kareem, A., Bergman, L.A., Johnson, E.A. and Klein, R.E. (1994), "Coupling tall buildings for control of response to wind", *6th International Conference on Structural Safety and Reliability*, Rotherdam, United Kingdom, 1553 -1560.
- Iwanami, K., Suzuki, K. and Seto, K. (1986), "Studies of the vibration control method of parallel structures", *Trans. JSME*, No. 86-0247A, 3063-3072.
- Jagadish, G., Kori and Jangid, R.S. (2008) "Semi-active friction dampers for seismic control of structures", *Smart Struct. Syst.*, **4**(4), 493-515.
- Jalayer, F. (2003), "Direct probabilistic seismic analysis: Implementation non-linear dynamic assessments", Ph.D. dissertation, Department of Civil And Environmental Engineering, Stanford University, Stanford.

- Jankowski, R. and Mahmoud, S. (2015), Earthquake-Induced Structural Pounding. Switzerland: Springer, ISBN: 978-3-319-16323-93.
- Katebi, J. and Mohammady Zadeh, S. (2016) "Time delay study for semi-active control of coupled adjacent structures using MR damper", *Struct. Eng. Mech.*, **58**(6), 1127-1143.
- Kima, J., Ryu, J. and Chung, L. (2006), "Seismic performance of structures connected by viscoelastic dampers", *Eng. Struct.*, **28**(2), 183-195.
- Klein, R.E., Cusano, C. and Stukel, J. (1972), "Investigation of a method to stabilize wind induced oscillations in large structures", New York: American Society of Mechanical Engineers.
- Lee, J. and Kim, J. (2015), "Seismic performance evaluation of moment frames with slit-friction hybrid dampers", *Earthq. Struct.*, **9**(6), 1291-1311.
- Lee, Y.J. and Moon, D.S. (2014), "A new methodology of the development of seismic fragility curves", *Smart Struct. Syst.*, **14**(5), 847-867.
- Luco, J.E. and Debarros, F.C.P. (1998), "Optimal damping between two adjacent elastic structures", *Earthq. Eng. Struct. D.*, **27**(7), 649-659.
- Lignos, D. (2008), "Sideway collapse of deteriorating structural systems under seismic excitations", Ph.D. dissertation, Department of Civil Engineering, Stanford University, Stanford.
- Nigdeli, S.M. and Bekdaş, G. (2014), "Optimum tuned mass damper approaches for adjacent structures", *Earthq. Struct.*, **7**(6), 1071-1091.
- Ng, C.L. and Xu, Y.L. (2004), "Experimental study on seismic response Mitigation of complex structure using passive friction damper", ANCER Annual Meeting, Networking of Young Earthquake Engineering Researchers and Professionals, The Sheraton Princess Kaiulani, Honolulu, Hawaii.
- Open system for Earthquake Engineering Simulation, OpenSees, (2008), Pacific Earthquake Engineering Research Center, <http://peer.berkeley.edu>
- Palacios-Quiñonero, F., Rubió-Massegú, J., Rossell, J.M. and Karimi, H.R. (2014), "Vibration control for adjacent structures using local state information", *Mechatronics*, **24**(4), 336-344.
- Pall, A.S., Marsh, C. and Fazio, P. (1980), "Friction joints for seismic control of large panel structures", *J. Restress. Concrete Inst.*, **25**(6), 38-61.
- Park, K.S. and Ok, A.Y. (2015), "Hybrid control approach for seismic coupling of two similar adjacent structures", *J. Sound Vib.*, **349**, 1-17.
- Patel, C.C. and Jangid, R.S. (2010a), "Seismic response of adjacent structures connected with Maxweel dampers", *Asian J. Civ. Eng. (Building and Housing)*, **11**(5), 585-603.
- Patel, C.C. and Jangid, R.S. (2010b), "Seismic response of dynamically similar adjacent structures connected with viscous dampers", *Inst. Environ. Sci. J., Part A: Civ. Struct. Eng.*, **3**(1), 1-13.
- Patel, C.C. and Jangid, R.S. (2010c), "Seismic response of adjacent structures connected with semi-active variable friction dampers", *Int. J. Acoust. Vib.*, **15**(1), 39-46.
- Patel, C.C. and Jangid, R.S. (2011), "Dynamic response of adjacent structures connected by friction damper", *Earthq. Struct.*, **2**(2), 149-169.
- Penzien, J. (1996), "Evaluation of building separation distance required to prevent pounding during strong earthquakes", *Earthq. Eng. Struct. D.*, **26**(8), 849-858.
- Pujari, N.N., Mandal, T.K., Ghosh, S. and Lala, S. (2013), "Optimization of IDA-based fragility curves", *The 11th International Conference on Structural Safety and Reliability*, Columbia University, New York.
- Setright, L.J.K. and Ward, I. (1976), "Anatomy of the motor car", Unknown publisher, pp. 166, ISBN 0-85613-230-6.
- Shrimali, M.K. and Dumne, S.M. (2008), "Seismic analysis of connected isolated buildings by VF dampers", *The 14th World Conference on Earthquake Engineering*, Beijing, China.
- Standard No. 2800. (2007), Iranian Code of Practice for Seismic Resistant Design of Buildings (3rd Ed.). Iran: Building and Housing Research Center.
- Uz, M.E. and Hadi, M.N.S. (2014), "Optimal design of semi active control for adjacent buildings connected by MR damper based on integrated fuzzy logic and multi-objective genetic algorithm", *Eng. Struct.*, **69**, 135-148.
- Vamvatsikos, D. and Cornell, C.A. (2005), "Developing efficient scalar and vector intensity measures for IDA capacity estimation by incorporating elastic spectral shape information", *Earthq. Eng. Struct. D.*, **34**(13), 1573-1600.
- Wang, J. and Taheri, H. (2014), "Seismic hazard assessment of the Tehran region", *Nat. Haz. Rev. J.*, **15**(2), 121-127.
- Xu, Y.L., He, Q. and Ko, J.M. (1999), "Dynamic response of damper-connected adjacent buildings under earthquake excitation", *J. Eng. Struct.*, **21**(2), 135-148.
- Yang, Z., Xu, Y.L. and Lu, X.L. (2003), "Experimental seismic study of adjacent buildings with fluid dampers", *J. Struct. Eng., ASCE*, **129**(2), 197-205.
- Zareian, F., Krawinkler, H., Ibarra, L. and Lignos, D. (2010), "Basic concepts and performance measures in prediction of collapse of buildings under earthquake ground motions", *Struct. Des. Tall Spec. Build.*, **19**(1-2), 167-181.
- Zhu, H., Ge, D. and Huang, X. (2011), "Optimum connecting dampers to reduce the seismic responses of parallel structures", *J. Sound Vib.*, **330**(19), 31-49.

CC